5

Nonlinear Phenomena during the Oxidation and Bromination of Pyrocatechol

Takashi Amemiya[1] and Jichang Wang[1,2]
[1]*Graduate School of Environment and Information Sciences, Yokohama National University, Yokohama, 240-8501*
[2]*Department of Chemistry and Biochemistry, University of Windsor, Windsor, Ontario, N9B 3P4*
[1]*Japan*
[2]*Canada*

1. Introduction

Many complex and interesting phenomena in nature are due to nonlinear interactions of the constituents (Nicolis & Prigogine, 1977; Ball, 1999; Morowitz, 2002). The study of nonlinear dynamical systems has achieved significant progress over the last four decades, which allows scientists to understand various rather complicated behaviors such as self-organization and pattern formation in the neuronal networks of brain (Scott Kelso, 1995). Unusual properties of reagents in far-from-equilibrium conditions and the prevalence of instability where small changes in initial conditions may lead to amplified effects have been documented more than a century ago, but those nonlinear chemical phenomena did not get much attention until late 1960s after the discovery of oscillatory behavior in a homogeneous solution reaction between acidic bromate and malonic acid in the presence of metal catalyst cerium (Field & Burgur, 1985; Scott, 1994; Epstein & Pojman 1998; Sagues & Epstein, 2003). The system is now commonly known as the Belousov-Zhabotinsky (BZ) reaction (Zaikin & Zhabotinsky, 1970; Field & Burger, 1985). Since then, the study of chemical oscillations and wave formation has blossomed, which led to the observation of various nonlinear spatiotemporal behaviours such as both simple and complex oscillations in a stirred system (Smoes, 1979; Györgi & Field, 1992; Wang et al., 1995 & 1996; Zhao et al., 2005), Turing pattern (Horváth et al., 2009), target and spiral waves in a two-dimensional reaction-diffusion medium (Zaikin & Zhabotinsky, 1970; Winfree, 1972; Yamaguchi et al., 1991; Steinbock et al., 1995; Kádár et al., 1998), and scroll waves in a 3-dimensional system (Welsh et al., 1983; Winfree, 1987; Jahnke et al., 1988; Amemiya et al., 1996). Understanding the onset of those exotic phenomena in chemical systems has provided important insight into the formation of similar behaviour in nature (Goldbeter, 1996; Dutt & Menzinger, 1999; Dhanarajan et al., 2002; Carlsson et al., 2006; Chiu et al., 2006).

As opposed to nonlinear systems in physical and biological areas, in which dynamic control parameters are often inaccessible or difficult to adjust, chemical reactions can be conveniently manipulated through adjusting the initial concentration of each reagent, temperature, or flow rate in a continuously flow stirred tank reactor (CSTR) (Epstein, 1989;

Source: Nonlinear Dynamics, Book edited by: Todd Evans,
ISBN 978-953-7619-61-9, pp. 366, January 2010, INTECH, Croatia, downloaded from SCIYO.COM

Mori et al., 1993; Amemiya et al., 2002). As a result, chemical media have played a very important role in gaining insights into various nonlinear behaviors encountered in nature (Nicolis & Prigogine, 1989; Sørensen et al., 1990; Kumli et al., 2003; Kurin-Csörgei et al., 2004; McIIwaine et al., 2006). Among existing chemical oscillators, the vast majority relies on a few elements that possess multiple oxidation states, such as halogens, sulfur and some transition metals. In 1978, Orbán and Körös carried out an extensive search to explore chemical oscillations in the oxidations of aromatic compounds by acidic bromate (Körös & Orbán, 1978; Orbán & Körös, 1978a; 1978b). Because of the absence of metal catalysts, systems reported by Orbàn and Körös in 1978 and discovered more recently by other groups have been frequently referred as uncatalyzed bromate oscillators (UBO) (Farage & Janjic, 1982; Szalai & Körös, 1998; Adamcikova et al., 2001). In general, reactions of UBOs represent the parallel running of oxidation and bromination of an organic substrate.

This chapter described nonlinear chemical kinetics in the bromate-pyrocatechol reaction with or without the presence of metal catalysts (Harati & Wang, 2008a; 2008b). The bromate-pyrocatechol reaction system was initially investigated by Orbàn and Körös in 1978 (Orbán & Körös, 1978a; 1978b). Unfortunately, no oscillatory behavior could be observed. The absence of spontaneous oscillations in the earlier attempt has been attributed to two major factors: First, the reaction between acidic bromate and pyrocatechol results in the production of bromine, which inhibits autocatalytic reactions; secondly, the oxidation product of pyrocatechol is a stable benzoquinone. As is shown in our recent reports, upon extensive search in the concentration phase space the bromate-pyrocatechol reaction was found to be capable of exhibiting spontaneous oscillations in a stirred batch system (Harati & Wang, 2008b). A phase diagram established in the bromate and pyrocatechol concentration space sheds light on why finding chemical oscillations in this chemical system is such a challenging task. Same as reported in other UBOs (Wang et al., 2001; Zhao & Wang, 2006 & 2007), the bromate-pyrocatechol reaction exhibits subtle responses to illumination, where, depending on the reaction conditions, either light-induced or light-quenched oscillatory phenomena could be observed. The influence of metal catalysts on the nonlinear dynamics of the bromate-pyrocatechol reaction was also discussed here.

2. Experimental observation of spontaneous oscillations

2.1 The uncatalyzed bromate-pyrocatechol reaction

Figure 1 presents three time series of the bromate-pyrocatechol (H_2Q) reaction performed under different initial concentrations of $NaBrO_3$: (a) 0.085 M, (b) 0.093 M, and (c) 0.095 M. Other reaction conditions are $[H_2Q]$ = 0.057 M and $[H_2SO_4]$ = 1.4 M. Details of the experimental procedure can be found in the original reports (Harati & Wang, 2007b). Shortly after mixing all chemicals together, Pt potential as seen in Fig. 1a exhibited clock reaction phenomenon, which was followed by gradual decrease for several hours. Phenomenologically, the excursion of the Pt potential was accompanied by a dramatic color change of the reaction solution from transparent to deep red. After the rapid color change, which has been observed in all of the following experiments, the red color gradually turned into yellow within the next two hours. Our experiments showed that for low bromate concentrations (<0.09 M), Pt potential of the system decreased monotonically after the initial excursion. Chemical oscillations were obtained when bromate concentration was increased to 0.093 M. Further increase of bromate concentration led to slightly irregular oscillations in Fig. 1c, where not only the amplitude but also the frequency of oscillation fluctuated. To

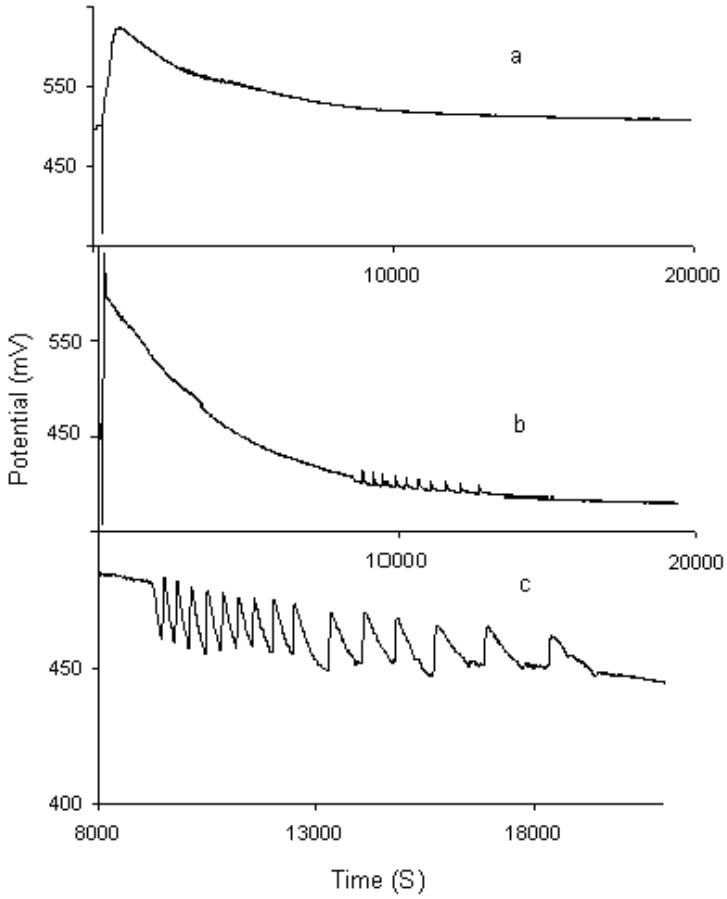

Fig. 1. Time series of the pyrocatechol – bromate reaction at different initial concentrations of bromate: (a) 0.085 M, (b) 0.093 M and (c) 0.095M. Other reaction conditions are $[H_2Q]$ = 0.057 M, and $[H_2SO_4]$ = 1.4 M.

show modulations in the oscillation frequency clearly, only the oscillation window is plotted in Fig. 1c, in which the long induction time period, similar to the ones plotted in Figs. 1a and 1b, is omitted. As bromate concentration was increased continuously, the system underwent reverse bifurcations leading the system back to non-oscillatory progress in time where the evolution of Pt potential was the same as that in Fig. 1a. For conditions employed in Fig. 1, spontaneous oscillations have been obtained when bromate concentration was between 0.09 and 0.11 M (Harati & Wang, 2007b).

Figure 2a plots the number of oscillation peak as a function of bromate concentration, where it increases with bromate concentration and then drops sharply to 0 as the system moves out of the oscillation window at the high bromate concentration. Fig. 2b illustrates that the induction time (IP) of these spontaneous oscillations grows monotonically with the increase

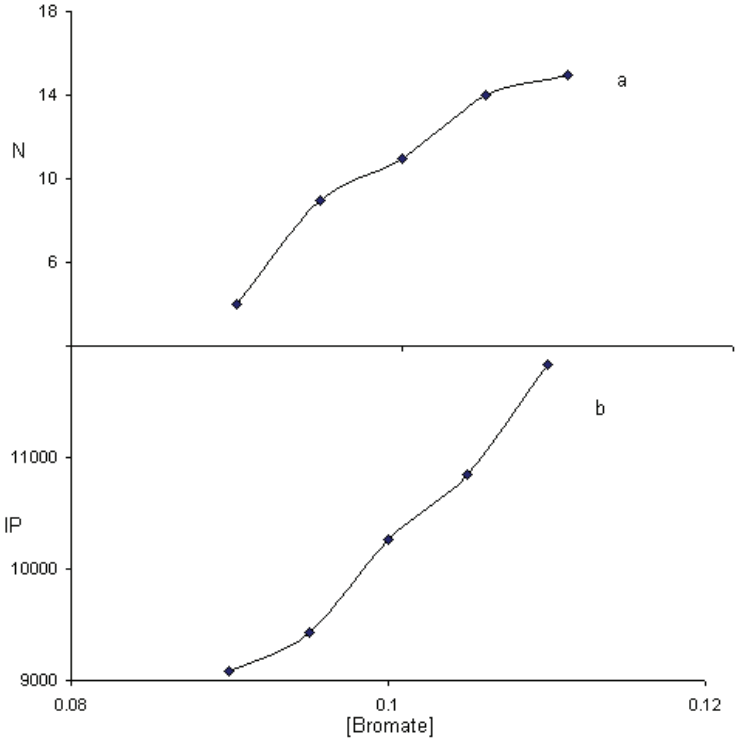

Fig. 2. Dependence of the number of oscillations (N) and induction period (IP) on the initial concentration of bromate. Other reaction conditions are $[H_2Q]$ = 0.057 M and $[H_2SO_4]$ = 1.2 M.

of bromate concentration. The extremely long induction seen here is similar to that reported in other uncatalyzed bromate oscillators (Farage & Janjic, 1982; Szalai & Körös, 1998; Adamcikova et al., 2001)

Figure 3 presents temporal evolutions of the bromate-H_2Q reaction under different initial concentrations of H_2Q: (a) 0.038 M, (b) 0.044 M, and (c) 0.047 M. In Fig. 3a Pt potential exhibits a clock reaction phenomenon, followed by a gradual decrease. This behavior is the same as seen at a low bromate concentration, where the clock variation of Pt potential is accompanied by a dramatic color change of the reaction solution. When H_2Q concentration was increased to 0.044 M in Fig. 3b, spontaneous oscillations took place at about 2 hours after the solution has turned into yellow. Further increase of H_2Q concentration also resulted in some irregularity in those transient oscillations such as the one shown in Fig. 3c. Again, to show details of the chemical oscillations time scale in Fig. 3c is different from that used in Figs. 3a and 3b. Within the oscillation window the induction time decreased monotonically with the increase of H_2Q concentration. On the other hand, the total number of oscillations increased rapidly as H_2Q concentration became larger than the lower bifurcation threshold and then decreased gradually as H_2Q concentration was increased further. The above results indicate that bromate and H_2Q have opposite effects on the oscillatory behavior.

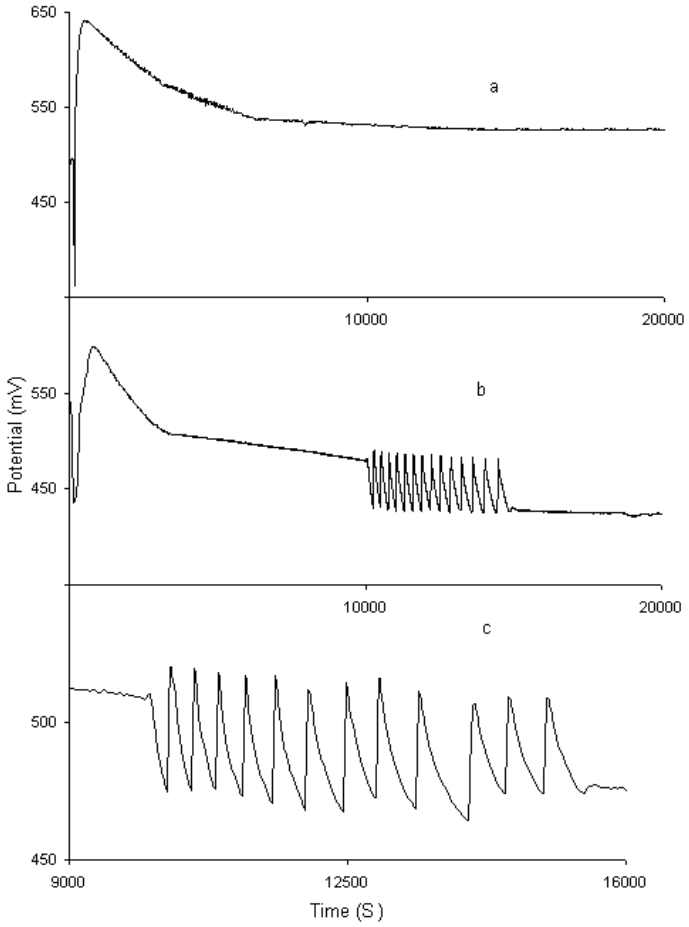

Fig. 3. Time series of the pyrocatechol – bromate reaction at different initial concentrations of pyrocatechol: (a) 0.038 M, (b) 0.044 M and (c) 0.047M. Other reaction conditions are $[NaBrO_3]$ = 0.085 M, and $[H_2SO_4]$ = 1.4 M

Figure 4 is a phase diagram in the pyrocatechol - bromate concentration plane, where filled triangles denote the conditions at which the system exhibits spontaneous oscillations. Here, the concentration of H_2SO_4 is fixed at 1.4 M. First glance of this phase diagram indicates that the oscillatory behavior exists over broad concentrations of pyrocatechol and bromate. However, at each given concentration of bromate (or pyrocatechol) there is only a narrow range of pyrocatechol (or bromate) concentration within that the system oscillates. This diagonal narrow band window sheds light on the difficulty of landing the initial conditions within such a window, when starting the experiments without existing information of this system.

Dependence of the above chemical oscillations on H_2SO_4 and bromate concentrations is summarized in Fig. 5, in which H_2Q concentration was fixed at 0.057 M. Filled triangles are

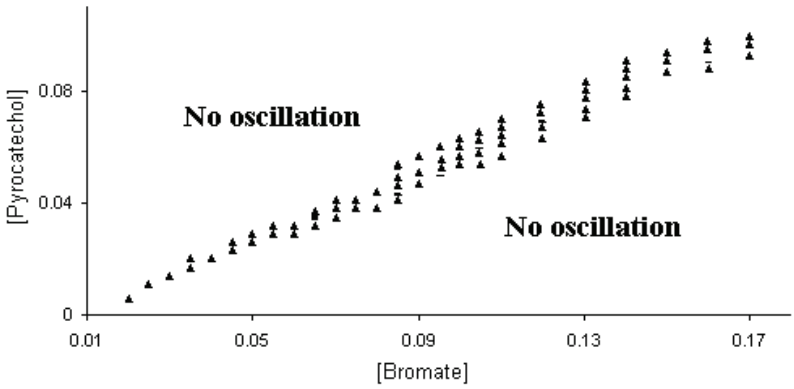

Fig. 4. Phase diagram of the bromate-pyrocatechol reaction in the pyrocatechol – bromate concentration plane. (▲) denotes where the system exhibits transient oscillations. Sulfuric acid concentration was fixed at 1.4 M.

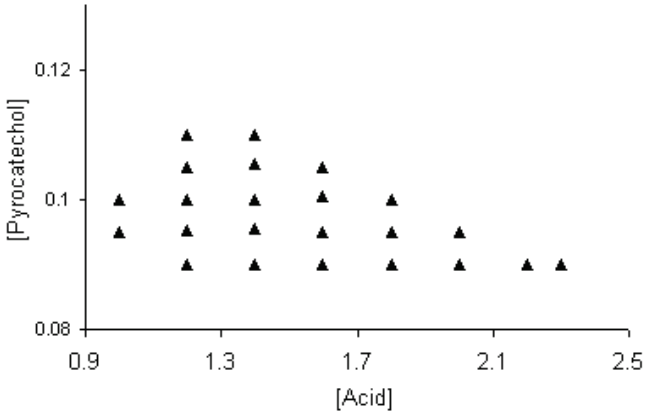

Fig. 5. Phase diagram of the bromate-pyrocatechol reaction in the bromate – H_2SO_4 concentration plane. (▲) denotes the conditions under which the system exhibits oscillations. The concentration of pyrocatechol is 0.057 M.

the conditions under which the system exhibits spontaneous oscillations. This phase diagram shows that when the concentration of H_2SO_4 is larger than 2.5 M or smaller than 0.9 M, no oscillations can be obtained regardless bromate concentration. On the other hand, the range of H_2SO_4 concentration over which the system exhibits spontaneous oscillations is broadened by lowering bromate concentration.

2.2 The ferroin-bromate-pyrocatechol reaction

Figure 6 presents time series of (a) the uncatalyzed and (b) ferroin-catalyzed bromate-pyrocatechol reactions. In the uncatalyzed system, the Pt potential decreased gradually after the initial excursion and then reached a plateau. In general, one might have considered that

this closed reaction is over. However, the Pt potential suddenly started oscillating after another two hours, and the oscillatory process lasted for longer than an hour with about 14 peaks. This result illustrates that under the conditions investigated here the uncatalyzed bromate-pyrocatechol is capable of exhibiting spontaneous oscillations. There is no periodic color change during the oscillation and thus the uncatalyzed system is deemed unsuitable for studying chemical waves in spatially extended media.

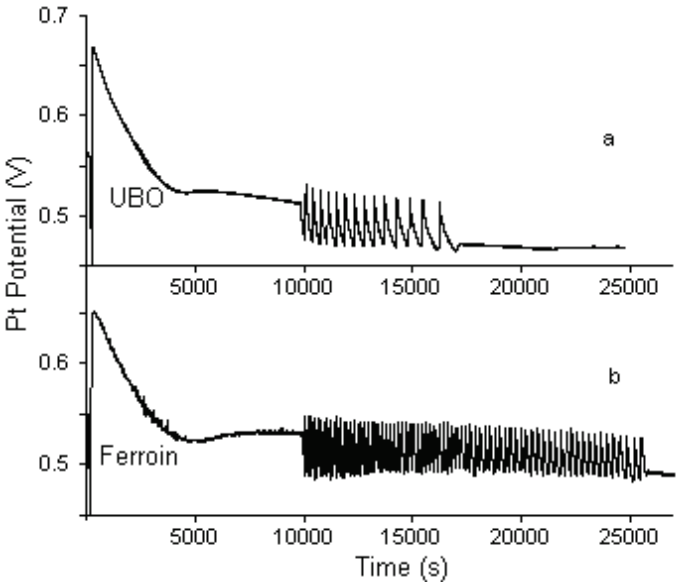

Fig. 6. Time series of the (a) uncatalyzed, and (b) ferroin-catalyzed bromate-pyrocatechol reaction. Other reaction conditions are: $[H_2SO_4]$ = 1.30 M, $[H_2Q]$ = 0.043 M and $[BrO_3^-]$ = 0.078 M. The concentration of ferroin is equal to 1.0 x 10^{-4} M in (b).

In Fig. 6b, when 1.0 x 10^{-4} M ferroin was added to the bromate-pyracatechol reaction, spontaneous oscillations commenced at about the same time as in the uncatalyzed system. However, there are significant changes in the frequency of oscillation and the total number of oscillations and both have been increased greatly. Notably, in this catalyzed system the oscillation lasted for longer than 4 hours. Our experiments illustrate that this system exhibits observable periodic color changes from yellowish to faint pink during the oscillatory window when the concentration of ferroin is above 1.0 x 10^{-4} M. Further increase of the concentration of ferroin results in a better contrast, but reduces the lifetime of the oscillatory period. Furthermore, when ferroin concentration is higher than 1.0 x 10^{-3} M no obvious color change could be seen in the stirred system. After oscillations in the ferroin-bromate-pyracatechol system stopped, the solution has a blue color if the concentration of ferroin added is above 1.0 x 10^{-3} M, or a pink color when the ferroin concentration is less than 5 × 10^{-4} M.

Figure 7 summarizes the dependence of the number of oscillations (N) and the induction time (IP) on the concentration of ferroin. There is a sharp increase in the number of oscillations at a very low concentration of ferroin (10^{-5} M), suggesting that the presence of small amounts of metal catalyst favours the oscillatory behaviour. As the amount of ferroin is increased, however, the number of oscillations decreases, which may be due to the

increased consumption of the reactants. Notably, ferroin shows a little effect on the induction time (IP), where increasing ferroin concentration to 0.002 M only reduces the IP by about 10 percent (Harati & Wang, 2008a).

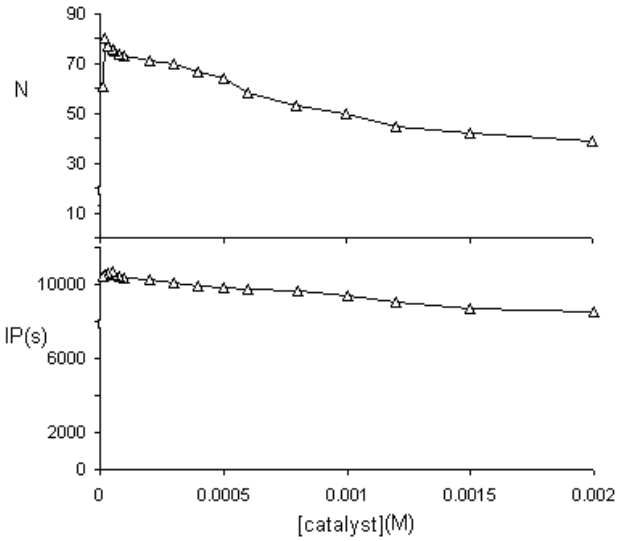

Fig. 7. Dependence of the number of oscillations (N) and induction period (IP) on the concentration of ferroin. Other reaction conditions are: $[H_2SO_4]$ = 1.30 M, $[BrO_3^-]$ = 0.078 M, and [pyrocatechol] = 0.043 M.

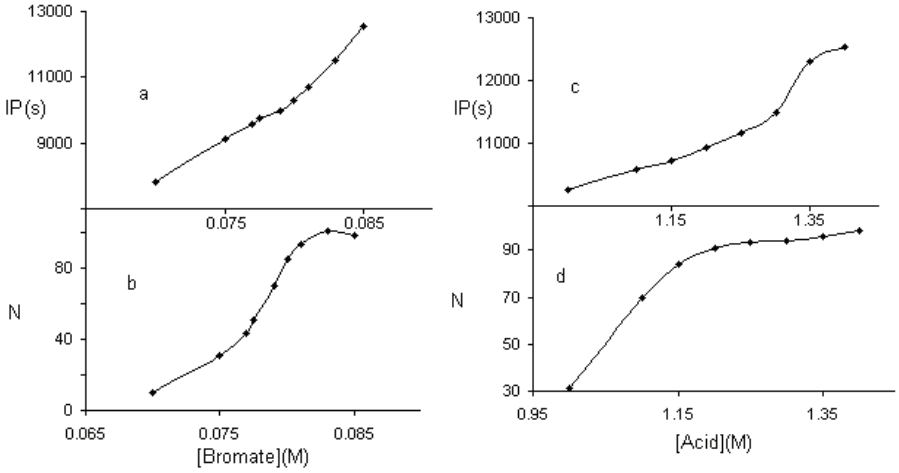

Fig. 8. Dependence of the number of oscillations (N) and induction time (IP) of the ferroin-catalyzed system on the concentration of bromate and sulfuric acid. Other reaction conditions are: $[H_2Q]$ = 0.044 M, [ferroin] = 1.0 x 10^{-4} M, and (a &b) $[H_2SO_4]$ = 1.40 M; (c&d) $[NaBrO_3]$ = 0.085 M.

Figure 8 plots, respectively, the number of oscillations (N) and induction time (IP) as a function of concentrations of bromate and sulfuric acid in the ferroin-bromate-pyrocatechol system, where the concentration of ferroin was fixed at 1.0 x 10^{-4} M. Figs. 8a and 8b show that increasing bromate concentration prolongs the induction period, which may arise from the production of larger amounts of bromine in the reaction solution. The number of peaks ascends first and then declines slightly with increasing bromate concentration. Under the conditions studied here, the concentration of bromate must be between 0.070 and 0.085 M for the system to show spontaneous oscillations. As shown in Figs. 8c and 8d, both N and IP increase monotonically with the increase of H_2SO_4 concentration. The system does not oscillate when the concentration of H_2SO_4 is higher than 1.4 M or lower than 1.0 M under the conditions studied.

Figure 9 is a phase diagram of the ferroin-catalyzed system in the pyrocatechol and bromate concentration plane, where (♦) indicates the conditions under which the system exhibits spontaneous oscillations. Similar to the situation of the uncatalyzed bromate-pyrocatechol reaction, the first glance of this figure suggests that the system is able to exhibit oscillatory dynamics over a broad range of bromate and pyrocatechol concentrations. However, at each given concentration of pyrocatechol (or bromate), the proper concentration of bromate (or pyrocatechol) is quite narrow. This narrow band shaped phase diagram suggests that nonlinear behavior of this catalyzed system is more sensitive to the ratio of $[H_2Q]/[BrO_3^-]$ than their absolute concentrations. In comparison to the uncatalyzed bromate-pyrocatechol system, the presence of ferroin does not change the shape of this phase diagram, but makes the area of the parameter window slightly larger, implicating that ferroin favors the oscillations.

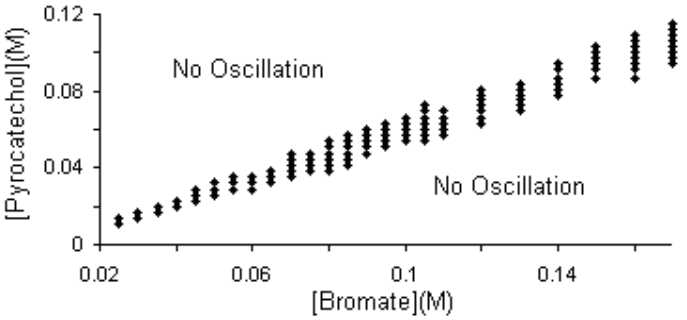

Fig. 9. Phase diagram of the ferroin-catalyzed reaction in the bromate–pyrocatechol concentration plane. (♦) denotes where the system exhibits simple periodic oscillations. The concentration of ferroin is 1.0 x 10^{-4} M.

Time series measured with a bromide selective electrode show that bromide concentration increases slowly during the long induction time and then starts oscillating (Harati & Wang, 2008b). It is similar to the behavior reported in earlier studies of the uncatalyzed bromate-1,4-cyclohexanedione and bromate-1,4-benzoquinone reactions (Szalai & Körös, 1998; Zhao & Wang, 2006), in which the accumulation of bromide precursors has been suggested to be responsible for the induction time. In this system, however, the initial addition of bromide, which leads to the rapid production of bromine and then causes the bromination of pyrocatechol, evidenced by mass spectrometry study (Harati & Wang, 2008b), does not

shorten the induction time. The slight decrease in the induction time observed at a very high bromide concentration may result from decreases in H_2Q and BrO_3^- concentrations due to reactions with bromine. The insensitivity of the induction time to the initial presence of brominated substrates suggests that the governing mechanism of this oscillator may be different from UBOs reported earlier.

2.3 The influence of Ce^{4+}/Ce^{3+} and Mn^{3+}/Mn^{2+}

It is well known that metal catalysts such as ferroin participate the autocatalytic reactions with bromine dioxide radicals (BrO_2*) and therefore redox potential of the metal catalyst in relative to the redox potential of $HBrO_2/BrO_2$* couple is an important parameter in determining the rate of the autocatalytic cycle, which in turn has significant effects on the overall reaction behavior. In the BZ reaction, four metal catalysts including ferroin, ruthenium, cerium and manganese can be oxidized by bromine dioxide radicals, in which the redox potential of $HBrO_2/BrO_2$* couple is larger than that of ferroin and ruthenium, but smaller than that of Ce^{4+}/Ce^{3+} and Mn^{3+}/Mn^{2+}. Therefore, it is anticipated that when cerium or manganese ions are introduced into the bromate-pyrocatechol reaction, behavior different from that achieved in the ferroin-bromate-pyrocatechol system may emerge. Figure 10 plots the number of oscilllations (N) and induction time (IP) of the catalyzed bromate-pyrocatechol reaction as a function of catalyst (i.e. Ce^{4+} and Mn^{2+}) concentration.

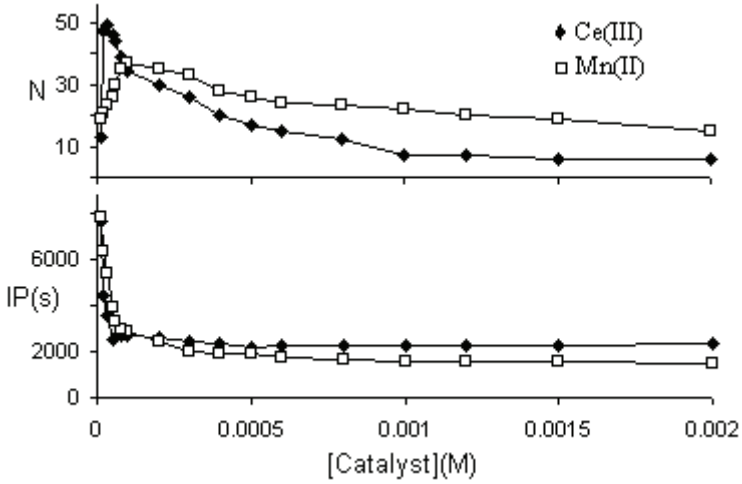

Fig. 10. Dependence of the number of oscillations (N) and induction time (IP) on the initial concentrations of cerium and menganese. Other reaction conditions are $[H_2SO_4]$ = 1.3 M, $[NaBrO_3]$ = 0.078 M, and $[H_2Q]$ = 0.043 M.

The sharp increase in the number of oscillations at the low concentration of cerium and manganese illustrates that the presence of a small amount of metal catalyst favours the oscillatory behaviour, similar to the case of ferroin. As the amount of catalyst (i.e. Ce^{4+} or Mn^{2+}) increases, however, the number of oscillations decreases rapidly. It could be due to the increased consumption of major reactants, in particular bromate. Overall, the effect of Mn^{2+} or Ce^{4+} on the number of oscillations was not as significant as ferroin, although they

doubled the number of peaks at an optimized condition. In contrast, the presence of a small amount of cerium or manganese dramatically reduced the induction time, where the induction time was shortened from about 3 hours in the uncatalyzed system to approximately half an hour when the concentration of manganese and cerium reached, respectively, 2.0×10^{-4} and 5.0×10^{-5} M. The IP became relative stable when the concentration of manganese or cerium was increased further.

When comparing with the time series of the ferroin system presented in Fig. 6b, for the cerium-catalyzed bromate-pyrocatechol reaction the Pt potential stayed flat after the initial excursion. The amplitude of oscillation became significantly larger than that of the uncatalyzed as well as the ferroin-catalyzed systems; but, there was no significant increase in the total number of oscillations when compared with the uncatalyzed system. Unlike the ferroin-catalyzed system, no periodic color change was achieved and thus is unfit for studying waves. A short induction time and large oscillation amplitude (> 300 mV), however, make the cerium-catalyzed system suitable for exploring temporal dynamics in a stirred system. In particular, oscillations in the cerium system have a broad shoulder which may potentially develop into complex oscillations. Times series of the Mn^{2+}-catalyzed bromate-pyrocatechol reaction is very similar to that of the cerium-catalyzed one, in which the Pt potential stayed flat after the initial excursion and the oscillation commenced much earlier than in the uncatalyzed system. The number of oscillations in the manganese system is also slightly larger than that of the uncatalyzed system. Overall, cerium and manganese, both have a redox potential above the redox potential of $HBrO_2/BrO_2$*, exhibit almost the same influence on the reaction behavior.

2.4 Photochemical behavior

Ferroin-catalyzed BZ reaction is insensitive to the illumination of visible light. As a result, the vast majority of existing studies on photosensitive chemical oscillators have been performed with ruthenium as the metal catalyst, despite that ruthenium complex is expensive and difficult to prepare. In Figure 11, the photosensitivity of the ferroin-catalyzed bromate-pyrocatechol reaction was examined, in which the concentration of ferroin was adjusted. As shown in Fig. 11a, when the system was exposed to light from the beginning of the reaction, spontaneous oscillations emerged earlier, where the induction time was shortened to about 6000 s, but the oscillatory process lasted for a shorter period of time. The system then evolved into non-oscillatory evolution. Interestingly, after turning off the illumination the Pt potential jumped to a higher value immediately and, more significantly, another batch of oscillations developed after a long induction time. The above result indicates that the ferroin-bromate-pyrocatechol reaction is photosensitive and influence of light in this ferroin-catalyzed system is subtle. On one hand, illumination seems to favor the oscillatory behavior by shortening the induction time, but it later quenches the oscillations.

In Fig. 11b the concentration of ferroin was doubled. When illuminated with the same light as in Fig. 11a from the beginning, no oscillation was achieved, except there was a sharp drop in the Pt potential at about the same time as that when oscillations occurred in Fig. 11a. After turning off the light, the un-illuminated system exhibited oscillatory behaviour with a long induction time. We have also applied illumination in the middle of the oscillatory window, in which a strong illumination such as 100 mW/cm^2 immediately quenched the oscillatory behaviour and oscillations revived shortly after reducing light intensity to a lower level such as 30 mW/cm^2. Interestingly, although ferroin itself is not a photosensitive

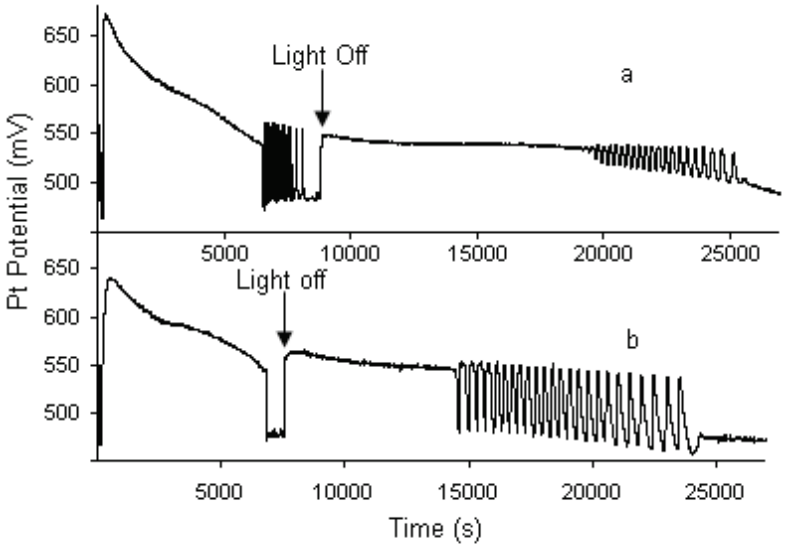

Fig. 11. Light effect on the bromate – pyrocatechol – ferroin reaction (a) and (b) light illuminating from the beginning with intensity equal to 70 mW/cm^2, under conditions [$NaBrO_3$] = 0.10 M, [H_2SO_4] = 1.40 M, [H_2Q] = 0.057 M, (a) [Ferroin] = 5.0×10^{-4} M, and (b) [Ferroin] = 1.0×10^{-3} M.

reagent, here its concentration nevertheless exhibits strong influence on the photoreaction behaviour of the bromate-pyrocatechol system. Carrying out similar experiments with the cerium- and manganese-catalyzed system under the otherwise the same reaction conditions showed little photosensitivity, in which no quenching behaviour could be obtained, although light did cause a visible decrease in the amplitude of oscillation.

3. Modelling

3.1 The model

To simulate the present experimental results, we employed the Orbán, Körös, and Noyes (OKN) mechanism (Orbán et al., 1979) proposed for uncatalyzed reaction of aromatic compounds with acidic bromate. The original OKN mechanism is composed of sixteen reaction steps, i.e., ten steps K1 – K10 in Scheme I and six steps K11 – K16 in Scheme II as listed in Table 1. We selected all ten reaction steps K1 – K10 from Scheme I and the first four reaction steps K11 – K14 in Scheme II. The reason behind such a selection is that all reaction steps in Scheme I as well as the first four reaction steps in Scheme II are suitable for an aromatic compound containing at least two phenolic groups such as pyrocatechol used in the present study.

Reaction steps K15 and K16 in Scheme II, on the other hand, suggest how phenol and its derivatives could be involved in the oscillatory reactions. There is no experimental evidence that pyrocatechol can be transformed into a substance of phenol type, we thus did not take into account reactions involving phenol and its derivatives. The model used in our

simulation consists of fourteen reaction steps K1 – K14, and eleven variables, BrO_3^-, Br^-, BrO_2*, $HBrO_2$, HOBr, Br*, Br_2, $HAr(OH)_2$, HAr(OH)O*, Q, and BrHQ, where $HAr(OH)_2$ is pyrocatechol abbreviated as H_2Q in the experimental section, HAr(OH)O* is pyrocatechol radical, $HArO_2$ is 1,2-benzoquinone and $BrAr(OH)_2$ is brominted pyrocatechol.

The simulation was carried out by numerical integration of the set of differential equations resulting from the application of the law of mass action to reactions K1 – K14 with the rate constants as listed in Table 1. The values of the rate constants for reactions K1 – K3, K5, K8 have already been determined in the studies of the BZ reaction, and those of all other reactions were either chosen from related work on the modified OKN mechanism by Herbine and Field (Herbine & Field, 1980) or adjusted to give good agreement between experimental results and simulations.

no.	reaction	rate constant		ref.
		forward	reverse	
Scheme I				
(K1)	$BrO_3^- + Br^- + 2H^+ \leftrightarrow HBrO_2 + HOBr$	$k_1 = 2.1\,[H^+]^2\ M^{-1}\ s^{-1}$	$k_{r1} = 1 \times 10^4\ M^{-1}\ s^{-1}$	*a*
(K2)	$HBrO_2 + Br^- + H^+ \rightarrow 2HOBr$	$k_2 = 2 \times 10^9\,[H^+]\ M^{-1}\ s^{-1}$		*a*
(K3)	$BrO_3^- + HBrO_2 + H^+ \leftrightarrow 2BrO_2^* + H_2O$	$k_3 = 1 \times 10^4\,[H^+]\ M^{-1}\ s^{-1}$	$k_{r3} = 2 \times 10^7\ M^{-1}\ s^{-1}$	*a*
(K4)	$BrO_2^* + HAr(OH)_2 \rightarrow HBrO_2 + HAr(OH)O^*$	$k_4 = 3 \times 10^2\ M^{-1}\ s^{-1}$		*a, b*
(K5)	$2HBrO_2 \rightarrow BrO_3^- + HOBr + H^+$	$k_5 = 4 \times 10^7\ M^{-1}\ s^{-1}$		*a*
(K6)	$HOBr + HAr(OH)O^* \leftrightarrow Br^* + HArO_2 + H_2O$	$k_6 = 2 \times 10^5\ M^{-1}\ s^{-1}$	$k_{r6} = 2 \times 10^2\ M^{-1}\ s^{-1}$	*a, b*
(K7)	$Br^* + HAr(OH)O^* \rightarrow Br^- + HArO_2 + H^+$	$k_7 = 4 \times 10^4\ M^{-1}\ s^{-1}$		*a, b*
(K8)	$HOBr + Br^- + H^+ \leftrightarrow Br_2 + H_2O$	$k_8 = 8 \times 10^9\,[H^+]\ M^{-1}\ s^{-1}$	$k_{r8} = 1.1 \times 10^2\ s^{-1}$	*a*
(K9)	$Br_2 + HAr(OH)_2 \rightarrow BrAr(OH)_2 + Br^- + H^+$	$k_9 = 7 \times 10^2\ M^{-1}\ s^{-1}$		*a, b*
(K10)	$HOBr + HAr(OH)_2 \rightarrow BrAr(OH)_2 + H_2O$	$k_{10} = 1\ M^{-1}\ s^{-1}$		*a, b*
Scheme II				
(K11)	$BrO_2^* + HAr(OH)O^* \rightarrow HBrO_2 + HArO_2$	$k_{11} = 5 \times 10^3\ M^{-1}\ s^{-1}$		*b*
(K12)	$Br^* + HAr(OH)_2 \rightarrow Br^- + HAr(OH)O^* + H^+$	$k_{12} = 1 \times 10^3\ M^{-1}\ s^{-1}$		*a, b*
(K13)	$HAr(OH)_2 + HArO_2 \leftrightarrow 2HAr(OH)O^*$	$k_{13} = 1 \times 10^{-2}\ M^{-1}\ s^{-1}$,	$k_{r13} = 1 \times 10^4\ M^{-1}\ s^{-1}$	*a, b*
(K14)	$2HAr(OH)O^* \rightarrow Ar_2(OH)_4$	$k_{14} = 1 \times 10^4\ M^{-1}\ s^{-1}$		*a, b*
(K15)	$BrO_2^* + HAr(OH) \rightarrow HArO^* + HBrO_2$			*c*
(K16)	$HArO^* + BrO_3^- + H^+ \rightarrow Ar(OH)_2 + BrO_2^*$			*c*

[a] Herbine and Field 1980. [b] Adustable parameter chosen to give a good fit to data. [c] Not used in the present model.

In this scheme, $HAr(OH)_2$ represents pyrocatechol compound containing two phenolic groups, HAr(OH)O* is the radical obtained by hydrogen atom abstraction, $HArO_2$ is the related quinone, $BrAr(OH)_2$ is the brominated derivative, and $Ar_2(OH)_4$ is the coupling product; HAr(OH) is phenol, HArO* is the hydrogen-atom abstracted radical, and $Ar(OH)_2$ is the product.

Table 1. OKN mechanism and rate constants used in the present simulation

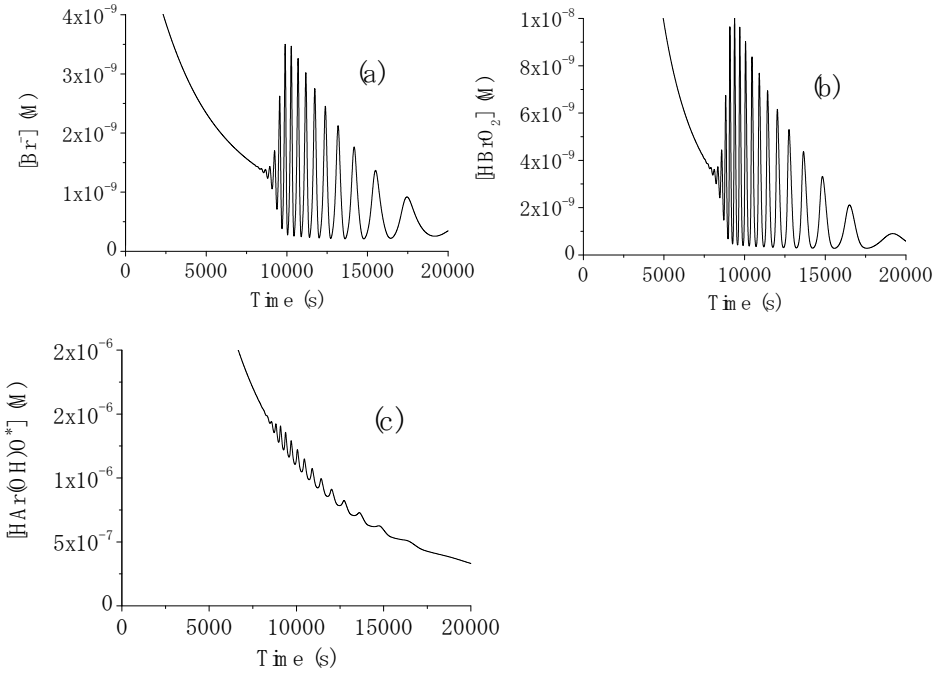

Fig. 12. Numerical simulations of oscillations in (a) Br^- (b) $HBrO_2$, and (c) pyrocatechol radical, HAr(OH)O*obtained from the present model K1 – K14 by using the rate constants listed in Table 1. The initilal concentraions were $[BrO_3^-]$=0.08 M, $[HAr(OH)_2]$=0.057 M, $[H_2SO_4]$=1.4 M, and $[Br^-]$=1.0 x 10^{-10} M; the other initial concentrations were zero.

3.2 Numerical results

Figure 12 shows oscillations in three (Br^-, $HBrO_2$, and HAr(OH)O*) of the eleven variables obtained in a simulation based on reactions K1 – K14 and the rate constant values listed in Table 1. The initial concentraions used in the simulation were $[NaBrO_3]$ = 0.08 M, $[HAr(OH)_2]$ = 0.057 M, $[H_2SO_4]$ = 1.4 M, and $[Br^-]$ = 1.0 x 10^{-10} M with the other initial concentrations to be zero with reference to those in the expreimental conditions as shown in Fig. 1. Other four variables, BrO_2*, Br*, HOBr, and Br_2, exhibited oscillations, whereas the rest variables, namely, BrO_3^-, $HAr(OH)_2$, $HArO_2$, and $BrAr(OH)_2$, did not exhibt oscillations in the present simulation.

Figure 13 shows oscillations in $[Br^-]$ at different initial concentrations of bromate: (a) 0.08 M, (b) 0.09 M, and (c) 0.1 M, with the same initial concentrations of $[HAr(OH)_2]$ = 0.057 M, $[H_2SO_4]$ = 1.4 M, and $[Br^-]$ = 1.0 x 10^{-10} M with reference to the experimental conditions as shown in Fig. 1. Although the concentration of bromate in the simulation is slightly smaller than that in the experiments, the agreement between experimentally obtained redox potential (Fig. 1) and simulated oscillations as shown in Figs. 12 and 13 is good. In particular, the induction period and the period of oscillations are similar in magnitude, as well as the degree of damping. The number of oscillations, and the prolonged period of

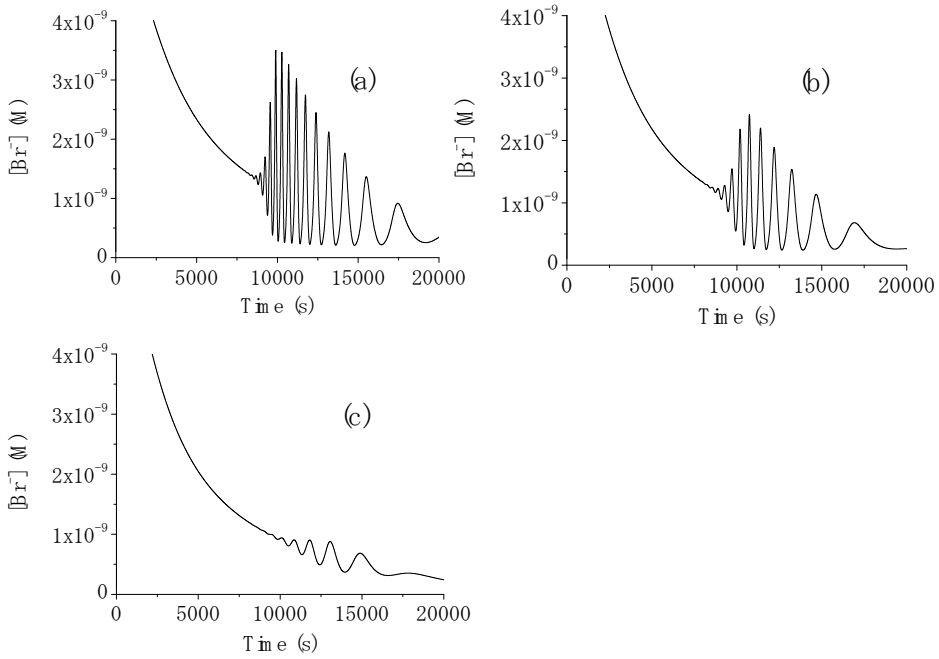

Fig. 13. Numerical simulations of the present model K1 – K14 at different initial concentrations of bromate: (a) 0.08 M, (b) 0.09 M, and (c) 0.1M. Other reaction conditions are $[HAr(OH)_2]$ = 0.057 M, $[H_2SO_4]$ = 1.4 M, and $[Br^-]$=1.0 x 10^{-10} M.

oscillations near the end of oscillations are also similar between experimental and simulated results as shown in Fig. 1 (c), Fig.3 (c), Fig.12, and Fig.13. The above simulation not only supports that the oscillatory phenomena seen in the batch system arises from intrinsic dynamics, but also provides a tempelate for further understanding the mechanism of this uncatalyzed bromate-pyrocatechol system.

While the above model is adequte in reproducing these spontaneous oscillations seen in experiments, the concentration range over which oscillations could be achieved is somehow different from what was determined in experiments. In the simulation, oscillatins were obtained in the range of 0.02 M < $[BrO_3^-]$ < 0.1 M with $[HAr(OH)_2]$ = 0.057 M and $[H_2SO_4]$ = 1.4 M in the present simuations, whereas no oscillation could be seen in experiments for the condition of $[BrO_3^-]$ < 0.085 M. This discrepancy of range of the reactant concentrations for exhibiting oscillations between experiments and simulations was also discerned for the concentration of $HAr(OH)_2$ under the conditions $[BrO_3^-]$ = 0.085 M and $[H_2SO_4]$ = 1.4 M: Oscillations were exhibited in the range of 3× 10^{-4} M < $[HAr(OH)_2]$ < 0.3 M in the simulation, whereas no oscillation could be observed in experiments under $[HAr(OH)_2]$ = 0.038 M as shown in Fig. 3 (a). The discrepancy in the suitable concentration range between experiment and simulation may arise from two sources: (1) the currently employed model may have skipped some of the unknown, but important reaction processes; (2) the rate

constants used in the calculation are too far away from their actual value. Note that those values were original proposed for the phenol system (Herbine & Field, 1980). To shed light on this issue, we have carefully adjusted the values of the adjustable rate constants in K4, K6, K7, K9 – K14, but so far no significant improvment was achhieved.

Two other sensitive properties that can help improve the modelling are the dependence of the number of oscillations (N) and induction period (IP) on the reaction conditions. In experiments, the N value increased monotonically from 4 to 15 as bromate concentration was increased and then oscillatory behavior suddenly disappeared with the further increase of bromate concentration. In contrast, in the simulation the number of oscillations decreased gradually from 17 to 9 and then oscillatory behavior disappeared as the result of increasing bromate concentration. On the positive side, IP values increased in both experiments and simulations with respect to the increase of bromate concentration, i.e., from 9100 s to 11700 s in the experiments, and from 8000 s to 9700 s in the simulations, respectively. We would like to note that the simulated IP values firstly decreased from 12600 s to 7500 s with increase in the initial concentration of bromate from 0.03 M to 0.06 M, then increased from 7600 s to 9700 s with increase in the bromate concentration from 0.07 M to 0.11 M.

3.3 Simplification of the model

In an attempt to catch the core of the above proposed model, we have examined the influence of each individual step on the oscillatory behavior and found that reaction step K12 in Scheme II is indispensable for oscillations under the present simulated conditions as shown in Fig. 12. Such an observation is different from what has been suggested earlier steps K1 to K10 would be sufficient to account for oscillations in the uncatalyzed bromate-aromatic compounds oscillators (Orbán et al., 1979). For the Scheme II, our calculations show that while setting one of the four rate constants k_{11} to k_{14} to zero; only when k_{12} was set to zero, no oscillation could be achieved. We further tested which reaction steps could be eliminated by setting the rate constants to zero under the condition of $k_{12} \neq 0$. The results are as follows: (i) when three rate constants k_{11}, k_{13}, k_{14} were simultaneously set to zero, no oscillation was exhibited, (ii) when only one of the three rate constants was set to zero, oscillation was observed in each case, and (iii) when two of the three rate constants were set to zero, oscillations were exhibited under the condition of either $k_{13} \neq 0$ (k_{11}=k_{14}=0) or $k_{14} \neq 0$ (k_{11}=k_{13}=0) with the range of the rate constants as $3.0 \times 10^3 < k_{13}$ (M^{-1} s^{-1}) $< 2.9 \times 10^4$ and $2.2 \times 10^3 < k_{14}$ (M^{-1} s^{-1}) $< 6.0 \times 10^4$, respectively. Thus our numerical investigation has concluded that oscillations can be exhibited with minimal reaction steps as ten reaction steps in Scheme I together with a combination of two reaction steps either K12 and K13 or K12 and K14 in Scheme II.

Fig. 14 presents time series calculated under different combinations of reaction steps from scheme II. This calculation result clearly illustrates that the oscillatory behavior is nearly identical when the reaction step K11 was eliminated. Meanwhile, eliminating K13 or K14 seems to have the same influence on total number of oscillations (Fig.14 (c) ,(d)). However, chemistry of the present reaction of aromatic compounds suggests that both reaction K13 and K14 are equally important (Orbán et al., 1979). The equilibrium of step K13 is well precedented, and equimolar mixtures of quinone and dihydroxybenzene are intensely colored, and the radical HAr(OH)O* may be responsible for the color changes observed during oscillations (Orbán et al., 1979). In addition, step K14 is said to explain the observed coupling products and to prevent the buildup of quinone for further oscillations (Orbán et al., 1979).

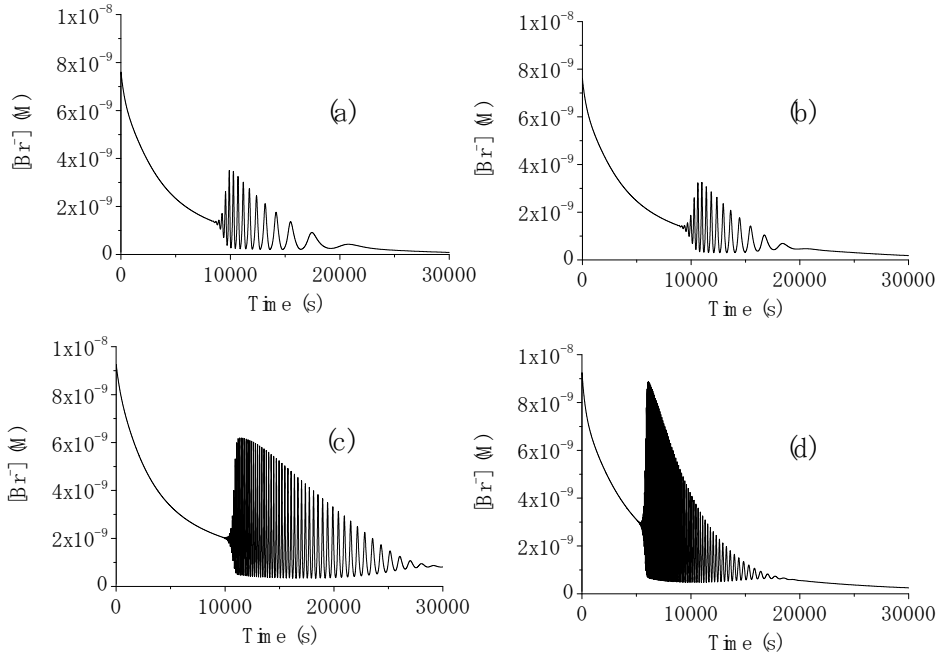

Fig. 14. Numerical simulations of the present model of K1 – K10 with different reaction steps in Scheme II: (a) K11 – K14, (b) K12 – K14, (c) K12 and K13, and (d) K12 and K14. The initilal concentraions were $[BrO_3^-]$ = 0.08 M, $[HAr(OH)_2]$ = 0.057 M, $[H_2SO_4]$ = 1.4 M, and $[Br^-]$ = 1.0 x 10^{-10} M as shown in Fig. 10. Note that the scales of x and y axes are different from those in Fig. 12.

In our numerical simulation, when we eliminated either step K13 or step K14, the simulated numerical results such as (i) the time series of oscillations, (ii) the initial concentration range of BrO_3^-, H_2SO_4, and $HAr(OH)_2$ for oscillations, and (iii) the dependence of the number of oscillations and induction period on the initial concentration of BrO_3^- became significantly different from those in experiments. In particular, the number of oscillations are too large under the above conditions as shown in Figs.14 (c) and (d). Such observation suggests that both K13 and K14 are important in the system studied here.

Consequently, we have concluded that the simplified model should include reaction steps K1 to K10 in Scheme I, and K12, K13, and K14 in Scheme II to reproduce the experimental results qualitatively.

3.4 Influence of reaction step K11 on the equilibrium of step K13

The numerical investigation presented in Fig. 14b suggests that reaction step K11 is not necessary for qualitatively reproducing the experimental oscillations. Besides, more positive reason for eliminatiing step K11 from the present model is that step K11 affects the range of rate constant of the equilibrium step K13 significantly. The equilibrium must lie well to the left (Orbán et al., 1979), i.e., the rate constant k_{r13} to the left must be much larger than that k_{13}

to the right. However, when we included step K11 in the model, we found no upper limit of the rate constant to the right; for instance, the rate constant can be more than 1.0×10^9 for the system to exhibit scillations under the conditions as shown in Fig.10. This value is already too large for the rate constant to the right, because we set the rate constant to the left to be 3.0×10^4 in the present simulations.

On the other hand, if we eliminated step K11 from the modelling, the range of the rate constant to the right was $0.007 < k_{13}$ (M^{-1} s^{-1}) < 0.03 for the system to exhibit oscillations, which seems to be reasonable for the equilibrium reaction step K13 to lie well to the left. Thus, this numerical analysis suggests that reaction step K11 should be eliminated from the present model.

4. Conclusions

This chapter reviewed recent studies on the nonlinear dynamics in the bromate-pyrocatechol reaction (Harati & Wang, 2008a and 2008b), which showed that spontaneous oscillations could be obtained under broad range of reaction conditions. However, when the concentration of bromate, the oxidant in this chemical oscillator, is fixed, the concentration of pyrocatechol within which the system could exhibit spontaneous oscillations is quite narrow. This accounts for the reason why earlier attempt of finding spontaneous oscillations in the bromate-pyrocatechol system had failed. As illustrated by phase diagrams in the concentration space, it is critical to keep the ratio of bromate/pyrocatechol within a proper range. From the viewpoint of nonlinear dynamics, bromate is a parameter which has a positive impact on the nonlinear feedback loop, where increasing bromate concentration enhances the autocatalytic cycle (i.e. nonlinear feedback). On the other hand, pyrocatechol involves in the production of bromide ions, a reagent which inhibits the autocatalytic process, where an increase of pyrocatechol concentration accelerates the production of bromide ions through reacting with such reagents as bromine molecules. The requirement of having a proper ratio of bromate/pyrocatechol reflects the need of having a balanced interaction between the activation cycle and inhibition process for the onset of oscillatory behaviour in this chemical system. If the above conclusion is rational, one can expect that the role that pyrocatechol reacts with bromine dioxide radicals to accomplish the autocatalytic cycle is less important than its involvement in bromide production in this uncatalyzed bromate oscillator, and therefore when a reagent such as metal catalyst is used to replace pyrocatechol to react with bromine dioxide radicals for completing the autocatalytic cycle, oscillations are still expected to be achievable. This is indeed the case. Experiments have shown spontaneous oscillations when cerium, ferroin or manganese ions were introduced into the bromate-pyrocatechol system.

Numerical simulations performed in this research show that the observed oscillatory phenomena could be qualitatively reproduced with a generic model proposed for non-catalyzed bromate oscillators. The simulation further indicates that while either two reaction steps K12 and K13 or K12 and K14 together with ten steps K1 – K10 in Scheme I in the OKN mechanism are sufficient to qualitatively reproduce oscillations, three steps K12, K13, and K14 with ten steps K1 – K10 are more realistic for representing the chemistry involving the oscillatory reactions, and also for reproducing oscillatory behaviors observed experimentally. The ratio of the rate constants for the equilibrium reaction K13 was a key reference to eliminate reaction step K11 from the original model. Although the present model still needs to be improved to reproduce the experimental results quantitatively, it has

given us a glimpse that the autocatalytic production of bromous acid could be modulated periodically even in the absence of a bromide ion precursor such as bromomalonic acid in the BZ reaction. Understanding the reproduction of bromide ion appears to be a key for deciphering the oscillatory mechanism for the family of uncatalyzed oscillatory reactions of substituted-aromatic compounds with bromate and should be given particularly attention in the future research.

5. Acknowledgements

This material is based on work supported by Natural Science and Engineering Research Council (NSERC), Canada, and Canada Foundation for Innovation (CFI). JW is grateful for an invitation fellowship from Japan Society for the Promotion of Science (JSPS).

6. References

Adamčíková, L.; Farbulová, Z. & Ševčík, P. (2001) *New J. Chem*. Vol. 25, 487-490.

Amemiya, T.; Kádár, S.; Kettunen, P. & Showalter K. (1996). *Phys. Rev. Lett*. Vol. 77, 3244-3247.

Amemiya, T.; Yamamoto, T.; Ohmori, T. & Yamaguchi, T. (2002) *J. Phys. Chem. A* Vol. 106, 612-620.

Ball P. (2001) *The Self-Made Tapestry: Pattern Formation in Nature*, Oxford University Press, ISBN-10: 0198502435.

Carlsson, P.; Zhdanov, V. P. & Skoglundh, M. (2006) *Phys. Chem. Chem. Phys*. Vol. 8, 2703–2706.

Chiu, A. W. L.; Jahromi, S. S.; Khosravani, H.; Carlen, L. P. & Bardakjian, L. B. (2006) *J. Neural Eng*. Vol. 3, 9-20.

Dhanarajan, A. P.; Misra, G. P. & Siegel, R. A. (2002) *J. Phys. Chem. A* Vol. 106, 8835-8838.

Dutt, A. K. & Menzinger, M. (1999) *J. Chem. Phys.* Vol. 110, 7591-7593.

Epstein, I. R. (1989). *J. Chem. Edu*. (1989) Vol. 66, 191-195.

Epstein, I. R. & Pojman, J. A. (1998) *An Introduction to Nonlinear Chemical Dynamics*, Oxford University Press, ISBN10: 0-19-509670-3, Oxford.

Farage, V. J. & Janjic, D. (1982) *Chem. Phys. Lett*. Vol. 88. 301-304.

Field, R. J. & Burger, M. (1985) (Eds.), *Oscillations and Traveling Waves in Chemical Systems*, Wiley-Interscience, ISBN-10: 0471893846, New York.

Goldbeter, A. (1996). *Biochemical Oscillations and Cellular Rhythms*, Cambridge University Press, ISBN 0-521-59946-6, Cambridge.

Györgi, L. & Field, R. J. (1992) *Nature* Vol. 355, 808-810.

Harati, M. & Wang, J. (2008a) *J. Phys. Chem. A* Vol. 112, 4241-4245.

Harati, M. & Wang, J. (2008b) *Z. Phys. Chem. A* Vol. 222, 997-1011.

Herbine, P. & Field, R. J. (1980) *J. Phys. Chem.* Vol. 84, 1330-1333.

Horváth, J.; Szalai, I. & De Kepper, P. (2009) *Science* Vol. 324, 772-775.

Jahnke, W.; Henze C. & Winfree, A. T. (1988) *Nature* Vol. 336, 662-665.

Kádár, S.; Wang, J. & Showalter, K. (1998) *Nature* Vol. 391, 770-743.

Körös, E. & Orbán, M. (1978) *Nature* Vol. 273, 371-372.

Kumli, P. I.; Burger, M.; Hauser, M. J. B.; Müller, S. C. & Nagy-Ungvarai, Z. (2003) *Phys. Chem. Chem. Phys.* Vol. 5, 5454-5458.

Kurin-Csörgei, K.; Epstein, I. R. & Orbán, M. (2004) *J. Phys. Chem. B* Vol. 108, 7352-7358.

McIIwaine, M.; Kovacs, K.; Scott, S. K. & Taylor, A. F. (2006) *Chem. Phys. Lett.* Vol. 417, 39-42.
Mori, Y.; Nakamichi Y.; Sekiguchi, T.; Okazaki, N.; Matsumura T. & Hanazaki, I. (1993) *Chem. Phys. Lett*. Vol. 211, 421-424.
Morowitz, H. J. (2002), *The Emergence of Everything: How the World Became Complex*, Oxford University Press, ISBN-13 978-0195135138, Oxford.
Nicolis, G. & Prigogine, I. (1977) *Self-Organization in Non-Equilibrium Systems*, Wiley, ISBN 10 - 0471024015.
Nicolis, G. & Prigogine, I. (1989) *Exploring Complexity*, FREEMAN, ISBN 0-7167-1859-6, New York.
Orbán, M. & Körös, E. (1978a) *J. Phys. Chem*. Vol. 82, 1672-1674.
Orbán, M. & Körös, E. (1978b) *React. Kinet. Catal. Lett.* Vol. 8, 273-276.
Orbán, M.; Körös, E. & Noyes, R. M. (1979) *J. Phys. Chem*. Vol. 83, 3056-3057.
Sagues, F. & Epstein, I. R. (2003) Nonlinear Chemical Dynamics, *Dalton Trans*., 1201-1217.
Scott Kelso J. A. (1995), *Dynamic Patterns: The self-organization of brain and behavior*, The MIT Press, ISBN-10: 0262611317, Cambridge, MA.
Scott, S. K. (1994) *Chemical Chaos*, Oxford University Press, ISBN 0-19-8556658-6, Oxford.
Smoes, M-L. *J. Chem. Phys*. (1979) Vol. 71, 4669-4679.
Sørensen, P. G.; Hynne, F. & Nielsen, K. (1990) *React. Kinet. Catal. Lett.* Vol. 42, 309-315.
Steinbock, O.; Kettunen, P. & Showalter K. (1995) *Science* Vol. 269, 1857-1860.
Straube, R.; Flockerzi, D.; Müller, S. C. & Hauser, M. J. B. (2005) *Phys. Rev. E*. Vol. 72, 066205-1 - 12.
Straube, R.; Müller, S. C. & Hauser, M. J. B. (2003) *Z. Phys. Chem*. Vol. 217, 1427-1442.
Szalai, I. & Körös, E. (1998) *J. Phys. Chem. A* Vol. 102, 6892-6897.
Yamaguchi, T.; Kuhnert, L.; Nagy-Ungvarai, Zs.; Müller, S. C. & Hess, B. (1991) *J. Phys. Chem*. Vol. 95, 5831-5837.
Vanag, V. K.; Míguez, D. G. & Epstein, I. R. (2006) *J. Chem. Phys*. Vol. 125, 194515:1-12.
Wang, J.; Hynne, F.; Sørensen, P. G. & Nielsen K. (1996) *J. Phys. Chem*. Vol. 100, 17593-17598.
Wang, J.; Sørensen, P. G. & Hynne, F. (1995) *Z. Phys. Chem*. Vol. 192, 63-76.
Wang, J.; Yadav, Y.; Zhao, B.; Gao, Q. & Huh, D. (2004) *J. Chem. Phys*. Vol. 121, 10138-10144.
Welsh, B. J.; Gomatam, J. & Burgess, A. E. *Nature* Vol. 304, 611-614.
Winfree, A. T. (1972) Science Vol. 175, 634-636.
Winfree, A. T. (1987) *When Time Breaks Down*, Princeton University Press, ISBN 0-691-02402-2, Princeton.
Witkowski, F. X.; Leon, L. J.; Penkoske, P. A.; Giles, W. R.; Spanol, M. L.; Ditto, W. L. & Winfree, A. T. (1998) *Nature* Vol 392, 78-82.
Zaikin, A. N. & Zhabotinsky, A. M. (1970) *Nature* Vol. 225, 535-537.
Zhao, J.; Chen, Y. & Wang, J. (2005) *J. Chem. Phys*. Vol. 122, 114514:1-7.
Zhao, B. & Wang, J. (2006) *Chem. Phys. Lett*. Vol. 430, 41-44.
Zhao, B. & Wang, J. (2007) *J. Photochem. Photobiol: Chemistry*, Vol. 192, 204-210.

Nonlinear Dynamics

Edited by Todd Evans

ISBN 978-953-7619-61-9
Hard cover, 366 pages
Publisher InTech
Published online 01, January, 2010
Published in print edition January, 2010

This volume covers a diverse collection of topics dealing with some of the fundamental concepts and applications embodied in the study of nonlinear dynamics. Each of the 15 chapters contained in this compendium generally fit into one of five topical areas: physics applications, nonlinear oscillators, electrical and mechanical systems, biological and behavioral applications or random processes. The authors of these chapters have contributed a stimulating cross section of new results, which provide a fertile spectrum of ideas that will inspire both seasoned researches and students.

InTech Europe
University Campus STeP Ri
Slavka Krautzeka 83/A
51000 Rijeka, Croatia
Phone: +385 (51) 770 447
Fax: +385 (51) 686 166
www.intechopen.com

InTech China
Unit 405, Office Block, Hotel Equatorial Shanghai
No.65, Yan An Road (West), Shanghai, 200040, China
中国上海市延安西路65号上海国际贵都大饭店办公楼405单元
Phone: +86-21-62489820
Fax: +86-21-62489821